

Synthesis of Functional Silver Nanoparticles and Microparticles with Modifiers and Evaluation of their Anti-cancer Activity on MDA-MB-453 Breast Cancer Cell Line

Mathew Kizhakkekara Joseph¹, Indhumathi Thangavel^{2,*}

¹Department of Biochemistry, Bharathiyar University, Coimbatore, Tamil Nadu, INDIA.

²Department of Biochemistry, N.G.P Arts and Science College, Coimbatore, Tamil Nadu, INDIA.

ABSTRACT

Background: One of the most noteworthy concerns in cancer theranostics in recent decades is the outcome of unique nanoparticles for diagnosing and treating purposes. In the current study, we used unripe *Garcinia cambogia* fruits to create silver nanoparticles utilizing a straightforward and environmentally friendly process. **Materials and Methods:** When exposed to fruit extract, the hydroalcoholic silver ions were decreased and stabilized over an extended period, leading to the biogenesis of silver nanoparticles with functionalized surfaces. These organically produced silver nanoparticles' properties were examined and characterized. **Results:** By measuring mitochondrial membrane potential, formation of the reactive oxygen species, the viability of the cell, and activities of caspase 3 and 9 against the MDA-MB-231 (Breast Cancer Cells), we were able to demonstrate the anti-cancer effects of these nanoparticles *in vitro*. The findings imply that the AgNPs have cytotoxic and apoptotic characteristics. **Conclusion:** According to the current research, AgNPs may aid in the creation of an effective anti-cancer drug, which could result in the creation of remarkable nanomedicine for treating different types of cancer.

Keywords: *Garcinia cambogia*, AgNPs, Cytotoxicity, MDA-MB-231, Caspase-3, Caspase-9.

Correspondence:

Prof. Indhumathi Thangavel

Professor, PG and Research Department of Biochemistry, N.G.P Arts and Science College, Coimbatore-641 048, Tamil Nadu, INDIA.
Email: indhumathi@drngpasc.ac.in

Received: 05-05-2023;

Revised: 14-05-2023;

Accepted: 12-06-2023.

INTRODUCTION

The field of nanotechnology has great promise for developing novel biotechnology and nanomedicine applications.¹ The usage of Silver Nanoparticles (AgNPs) as an antibacterial substance in clothing, bandages, and household appliances like refrigerators and washing machines has grown significantly. Nanosilver is one of many nanoproducts, and it is one of the most well-known. Antibacterial, antifungal, antioxidant, and anti-inflammatory activities have all been attributed to AgNPs.² The most promising area for developing innovative types of nanomaterials for biomedical purposes is nanobiotechnology. For the green synthesis of NPs, many natural resources like plants, products derived from plants, bacteria, viruses, fungi, yeast, and algae have been used.

Because they are simple to handle and can be genetically altered, bacteria and fungi are the most frequently chosen method.

Traditional approaches, such as physical and chemical ones, are employed to produce NPs in general. Physical procedures have a lower yield, whilst chemical processes are environmentally hazardous due to the use of harmful chemical-reducing agents. Biological approaches, on the other hand, employ enzymatic reduction of AgNPs, which provides greater power for the synthesised NPs.³ Because particle form is critical in many medicinal applications, the biological system manages particle dimensions and external characteristics better than physical and chemical methods of NPs formation. Adjusting factors including types of microorganisms, microbial cell growth phase, growth medium, pH, temperature, synthesis conditions, reaction time, concentrations of the substrate, reference compound of target NPs, and the acquisition of nontarget ions may allow for adequate management of particle length and their monodispersity.⁴

The NPs are occasionally covered with a layer of lipids, which confirms physiological stability and solubility, both are required for biomedical importance and the blockage of further synthetic procedures, making beneficial biological techniques. Biological approaches also have stability, cost-effectiveness, biocompatibility, significant dispersity, and minimal toxicity. As a result, it is critical to seek other sources of AgNPs for plant-based synthesis.



DOI: 10.5530/fra.2023.1.4

Copyright Information :

Copyright Author (s) 2023 Distributed under Creative Commons CC-BY 4.0

Publishing Partner : EManuscript Tech. [www.emanuscript.in]

The leading factor in global mortality is cancer. The second most frequent malignancy among women to cause death is breast cancer. Despite initially responding to chemotherapy, many cancers eventually develop resistance. Because the chemotherapeutic and chemopreventive drugs currently on the market have unfavourable side effects, it is essential to find a biocompatible and affordable cancer treatment method. Anaemia and, most importantly, the development of cellular resistance are among the costly and well-documented adverse effects of the cytotoxic drugs used to treat it. To overcome these constraints, alternate therapy or drugs must be found.⁵ Nanotechnology has contributed to a variety of applications, including medicines, catalysis, biosensing devices, and biomedicine, because of its easy production process, quality control, and biocompatibility. It is already used in clinical practice for wound healing and antimicrobial applications. AgNPs have shown *in vitro* to activate the apoptotic pathway via the formation of free oxygen radicals, resulting in anti-cancer, antiangiogenic and antiproliferative properties.⁶

Because of the extraordinary characteristics and significant therapeutic possibility in treating different kinds of illnesses. AgNPs are the developing nanoproducts in the area of nanomedicine that are attracting a lot of interest.⁷ AgNPs did not merely interpret the normal activities of cells and even influence membrane integrity, initiating several apoptotic signaling pathways in mammalian cells.⁸ AgNPs enhanced the formation of Reactive Oxygen Species (ROS) and activated the c-Jun N-terminal kinase pathway, causing death in murine embryonic fibroblasts cells (NIH 3T3).⁹ The effectiveness and drawbacks of several cytotoxic drugs employed in the remedy of breast cancer, including cisplatin, doxorubicin, etc., are unknown.¹⁰ Therefore, it is essential to discover new cancer therapeutics that are both affordable and biocompatible.

In this study, we first synthesized AgNPs from the fruit extract of the *Garcinia cambogia* plant. These AgNPs were subsequently characterized by X-ray diffraction, the Duckworth-Lewis-Stern method, atomic force microscopy, and Energy Dispersive X-ray spectroscopy. The cytotoxic impact of AgNPs on human breast cancer cells (MDA-MB-231) was also investigated. Third, measures of Mitochondrial Membrane Potential (MMP), ROS generation, and caspase-3 and caspase-9 activity were used to evaluate the likely mechanism of AgNP-induced cell death.

MATERIALS AND METHODS

Reagents

All of the chemicals were of analytical grade and could be employed right away without further purification. All chemicals were prepared using deionized water.

Preparation of Extracts

Harvesting and Identification of *G. cambogia*

The plant was gathered from several conservatories in Tamil Nadu, India, between February and June 2022.

Cleaning and Drying

Plants were split into fruit portions, and after the common dirt was removed, drinkable water was utilized to rinse the plants. To minimize humidity buildup, the plant material was parched at ambient temperature in the lack of light using printing paper that was replaced every 24 hr.

Extracts Preparation

Dry *Garcinia cambogia* fruit can be used as a test sample, crushed and filled in a porous cellulose thimble. PHF and 70% ethanol are added to a Soxhlet extractor and condenser, which evaporate for 4 hr. The extract is kept in the refrigerator for future use.

Synthesis of AgNPs

A previously described technique was used to create AgNPs.⁹ A typical reaction involved combining 1 mg/mL hydroalcoholic *G. cambogia* extract with a 1 mM AgNO₃ aqueous solution and allowing the combination to remain at ordinary room temperature for one day. The synthesis was noticed by employing UV-visible spectroscopy. After 12 hr in the presence of silver nitrate, the colouration turned white. The reduction of AgNO₃ to Ag was caused by phytochemicals identified in the extracts and this is acting as reducing as well as capping agents. To test the durability of synthetic AgNO₃ and the same was maintained at 4°C until further study.

Characterization of AgNPs

UV-visible spectra of the individual AgNPs were observed by employing a double-beam spectrophotometer (Shimadzu 1800 UV-visible spectrophotometer). Between 200 and 800 nanometers of wavelength were used to measure the absorbance. Shimadzu's (FTIR8400S) transmission mode was used to record Fourier transform infrared spectra in the 400–4000 cm⁻¹ range. Elemental analysis of the generated AgNPs was conducted by employing energy-dispersive X-ray spectroscopy in conjunction with field emission scanning electron microscopy (JEOL JSM-7600F). Transmission electron microscopy (TEM; JEM-1200EX; JEOL, Japan) was employed to analyse the dimensions and form of AgNPs. The TEM picture was captured at a 300 kV accelerating voltage. The produced AgNPs were investigated under a scanning electron microscope (SEM, LEO SEM 1450VP, UK) to determine their shapes and morphologies. Atomic Force Microscope (AFM) through drop-casting a liquid sample containing silver nanoparticles onto a glass substrate and letting the solvent evaporate before the examination. Utilizing a Malvern particle

size analyzer, the Dynamic Light Scattering (DLS) approach is applied.

Cell culture

MDA-MB-231 were generously supplied by the National Centre for Cell Science in Pune. The same was developed and held at the temperature of 37°C in 5% CO₂ using DMEM containing 10% foetal calf serum and 1% streptomycin and penicillin. Unless otherwise specified, all investigations were carried out in six-well plates. Before the experiments, cells were implanted at a density of 1106 cells per well onto the plates and incubated for 24 hr. The cells were rinsed in PBS (phosphate-buffered saline; pH 7.4) before being cultivated in new media having varying amounts of dissolved AgNPs.

Cell-viability assay

The viability of the cell was estimated by utilizing the 3-[4,5-dimethylthiazol-2-yl]-2,5-diphenyltetrazolium bromide dye-reduction (MTT) test to assess the cytotoxic impact of the synthesised AgNPs at different dosages. To plate cells, 96-well flat-bottom culture plates using varied AgNP dosages (0-10 g/mL) were utilized. Every culture was kept alive for 24 hr in a humid incubator at a temperature of 37°C. After the initial 24 hr of incubation (37°C, 5% CO₂ with moist conditions), 10 L of MTT (5 mg/mL in PBS) was mixed in each well, and the plate was placed for an additional 4 hr at a temperature of 37°C. After dissolving the formazan in 100 L of dimethyl sulfoxide with mild vibration at a temperature of 37°C, the absorbance at 595 nm was estimated using an enzyme-linked immunosorbent assay reader (SpectraMax; USA). Then, for AgNP concentrations that resulted in a 50% drop in cell viability, IC₅₀ [half-maximal inhibitory concentration] was estimated.

$$\% \text{ of Growth Inhibition} = (\text{Control OD} - \text{Treated OD} / \text{Control OD}) \times 100$$

Analysis of MMP

MMPs that cause apoptosis in AgNP-given MDA-MB-231 cells have been quantified by rhodamine-123 staining. The cells were loaded with the required amount of biosynthesized AgNPs for 24 hr, during which time 1 mM rhodamine 123 was provided, and the cells were then set for 15 min to measure mitochondrial dysfunction. As controls, cells that had not been treated were employed.

Determination of ROS

To measure intracellular ROS, the fluorescent chemical 2',7'-dichlorofluorescein (DCF) was utilized, which is formed by the intracellular peroxide-dependent oxidation of 2',7'-dichlorodihydrofluorescein diacetate (DCFH-DA). 49 cells were implanted into 24-well plates at the density of 5104 cells per well and cultivated for one day. Behind washing the cells double

with PBS, a new medium comprising 6 g/mL of AgNPs or 1 mM of doxorubicin was mixed. After that, the cells were cultured for one day. Cells were feted for 30 min at 37°C with 20 M DCFH-DA as a control. After washing the cells with PBS and adding 2 mL of PBS to individual wells, the fluorescence intensity was measured using a spectrofluorometer (Gemini EM; Molecular Devices) with excitation at 485 nm and emission at 530 nm. 5 mM N-acetyl-L-cysteine (NAC) was administered to cells cultivated in 24-well plates for one day before they were subjected to 6 g/mL AgNPs or 1 M doxorubicin for 12 hr. The cells were incubated for 30 min at 37°C behind the addition of DCFH-DA (20 M) to measure any changes in DCF fluorescence.

Assessment of caspase-3 and caspase-9 activities

After being loaded with AgNPs, the apoptosis proteins caspase-3 and caspase-9, as well as their activities, were investigated in MDA-MB-231. The synthesised AgNPs were applied to the cells for 24 hr. The treated and control cells were then used to produce total proteins. An immunoblotting analysis was done to determine the apoptotic protein activity after protein extraction.

RESULTS AND DISCUSSION

AgNPs synthesis

In the present investigation, we tried to synthesize AgNPs using *Garcinia cambogia* extract. Figure 1 displays tubes containing *Garcinia cambogia* extract, silver nitrate, and extract after a 24 hr reaction with Ag⁺ ions. Before reacting with the silver ions, the extract was seen to have a brownish hue; when the reaction was complete, the hue turned white. The stimulation of surface plasmon vibrations in the NPs caused a yellowish-white colour to develop in the extract-containing solution, which was a definite sign that AgNPs had formed in the reaction mixture.¹¹ Given the colour change, *Garcinia cambogia* extract may be employed as a reducing and stabilising substance for AgNP manufacturing and synthesis

Description of AgNPs by UV-visible Spectroscopy

UV-visible spectroscopy was used to describe the produced AgNPs. To characterize NPs, UV-visible spectroscopy is a crucial and useful approach.¹² AgNPs' UV-visible absorption spectra were measured in the 300–600 nm range. The AgNPs made using *Garcinia cambogia* mycelia extract showed a robust and comprehensive surface plasmon peak at 420 nm (Figure 2). The development of exceptionally stable AgNPs with no signs of flocculation even after three months is indicated by the firm surface plasmon resonance centered at 440 nm. The band at 440 nm shows that there was no aggregation and that the particles were evenly distributed. The proteins acting as capping agents in the mushroom extract may be the cause of the NP solution's long-term stability.¹³ Since the power of the surface plasmon peak is instantly correlated to the thickness of the NPs, the

results of our further investigation into the role of duration for the synthesis of AgNPs point to the formation of AgNPs as the reaction progresses as evidenced by the steady increasing peak intensity with increasing reaction time. The reaction reached its peak strength after 24 hr, which demonstrates that the Ag^+ ions were completely reduced. The reaction mixture's deep dark hue adds more evidence that Ag^+ ions were completely reduced and AgNPs were created.

FT-IR analysis

To learn more about the extract ingredients involved in reducing Ag^{+3} to Ag and/or stabilizing AgNPs, both extracts and AgNPs had their FT-IR spectra taken. The FT-IR ranges are given in Figure 3. The FT-IR ranges of extracts and AgNPs are significantly the same. Even though the spectra of extracts and AgNPs were comparable, several absorption peaks changed in location and/or strength. The reduction in comparable intensities and absorption frequencies at 3369 cm^{-1} and 3376 cm^{-1} ; 1738 cm^{-1} , 1633 cm^{-1} , and 1077 cm^{-1} indicates that biomolecules having O-H groups (polyols), -C=O groups (flavonoids), -C-N and -N-H (proteins), and -C=O and -C=O groups are involved in bioreduction and/or NP stabilization. The peaks between 2356 cm^{-1} and 2357 cm^{-1} are present because of atmospheric carbon dioxide.

XRD investigation of AgNPs

XRD was then used to establish the crystalline character of the synthesised AgNPs. There are 2 significant XRD peaks were seen, compared to the planes of (111) and (200) at 38.28° and 44.38° , respectively, showing that the AgNPs are crystalline (Figure 4). The nanoparticles made from *Garcinia cambogia* extract have XRD spectra that point to the production of metallic silver. The Scherer equation was used to determine the average crystallite size by utilizing the width of the (111) peak. The predicted intermediate size was discovered to be 3 nm and agrees with the particle dimension determined from a TEM picture of AgNPs made with an extract of *Garcinia cambogia*.

Additionally, Bragg peaks indicative of face-centered cubic AgNPs (shown by stars), and other unassigned peaks (indicated by stars mark) were seen, indicating the bioorganic phase

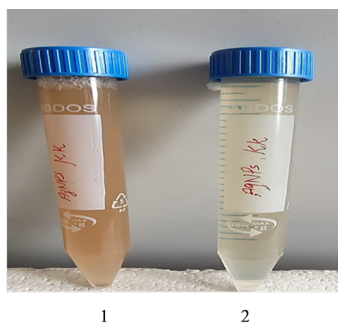


Figure 1: Synthesis of Silver Nanoparticles (AgNPs) using *Garcinia cambogia* extract. The photo shows containers with samples of AgNO_3 (1), *Garcinia cambogia* extract (2), AgNO_3 with the *Garcinia cambogia* extract.

crystallized on the outside of the AgNPs. The outcomes of the present study are agreeing with previous investigations showing the synthesis of AgNPs from an edible mushroom extract and geranium leaf extract.¹⁴ An extreme diffraction peak at 2 angles of 57.3° , which they attributed to chloride ions used in the cell filtrate creation as well as probable residual from a biomass extract. The reaction of the silver nitrate resulted in the formation of three more peaks.

Dynamic light scattering for size-distribution

A size distribution investigation was carried out utilizing dynamic light scattering in a hydroalcoholic solution to find out the moderate size of AgNPs. Figure 5 demonstrates that the generated AgNPs using *Garcinia cambogia* extract had a moderate particle dimension of 3 nm. The DLS data revealed that the majority of the species in solution were single, uniform-sized species with sizes varying from 2 and 10 nm, with a low Polydispersity Index (PI) of 0.175. *Verticillium* exposure reduced the metal ions in the aqueous AgNO_3 solution and resulted in the creation of AgNPs with a 25 nm diameter. AgNPs were reported to be produced via cell-associated biosynthesis in *Fusarium oxysporum*, and the particles with a length range between 5 and 15 nm.¹⁵

Size and morphology analysis of AgNPs by SEM and TEM

The shape, size, and morphology of the AgNPs were further characterized by employing SEM (Figure 6a) and TEM (Figure 6b) examinations. This demonstrates that the majority of AgNPs have mainly spherical with a triangular shape structure and a moderate size of 3 nm. To confirm the findings from the DLS investigation, AgNPs were further characterized by TEM to analyse their size and morphology. Figures 6a-b is a representative TEM picture that shows well-dispersed, noticeably uniform, and spherical particles. According to the TEM study, the moderate size of the particles created by *Garcinia cambogia* was around 2-3 nm. In TEM images, a sizable percentage of essentially spherical AgNPs in the 3 nm range were visible. The triangular-shaped spheres were reasonably homogeneous in size and agreed with the DLS results. AgNPs made from *Garcinia cambogia* extract had an average size of 3 nm, according to a combined investigation of

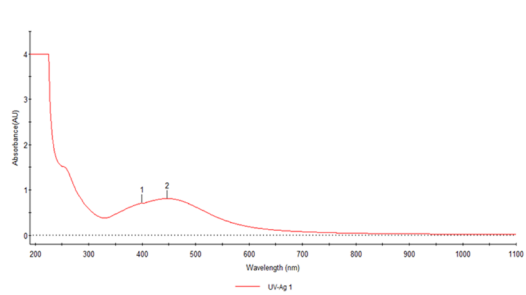


Figure 2: The Ultraviolet-visible Spectra of Silver Nanoparticles (AgNPs). The absorption spectra of AgNPs exhibited a strong broad peak at 440 nm, and observation of this band was attributed to surface Plasmon resonance of the particles.

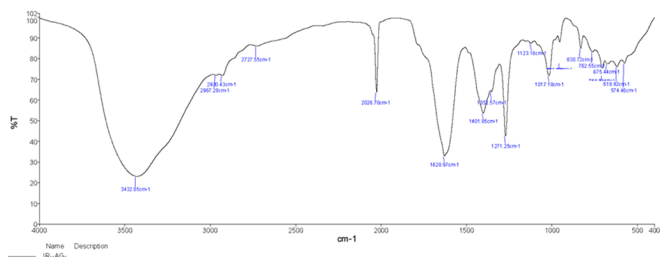


Figure 3: FT-IR spectra of the AgNPs/GC.

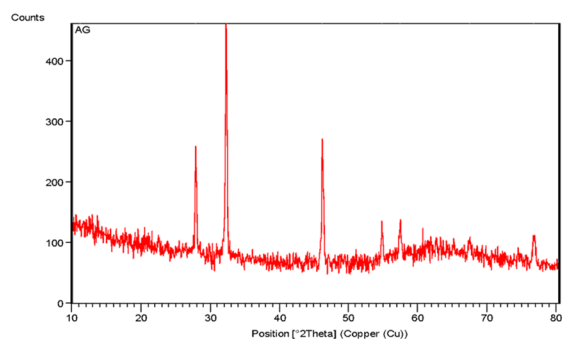


Figure 4: X-ray diffraction pattern of the Silver Nanoparticles (AgNPs) derived from *Garcinia cambogia* extract. The diffractions at 38.28° and 44.38° 2θ can be indexed to the (111) and (200) planes of the face-centered cubic AgNPs, respectively.

Intensity Distribution

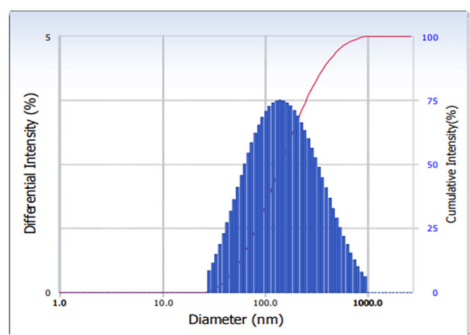
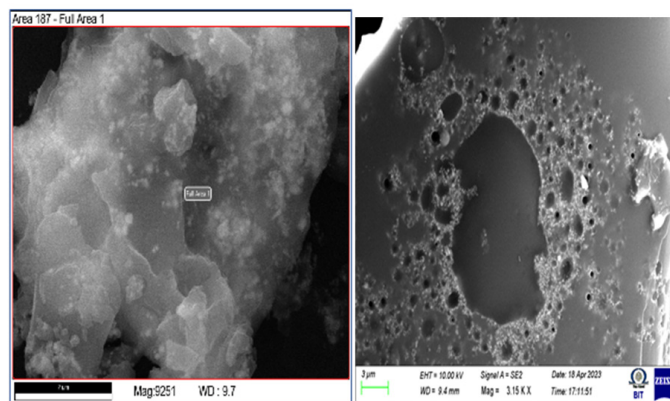


Figure 5: Size-distribution analysis by dynamic light scattering. The particle size-distribution analysis revealed that particle size was about 3 nm.

SEM, DLS, and TEM. A productive and dependable method for increasing a material's biocompatibility is to reduce the size of its particles.¹⁶

EDX examination

As seen in Figure 7, the compositional analysis of AgNPs was investigated utilizing EDX analysis. For AgNPs/GC, the EDX spectrum clearly showed the presence of Ag at 1.32 keV. AgNPs/GC revealed that the elemental composition of Ag was 98.68% and 98.68%, respectively. Other faint or moderate signals, such as C, O, Ca, K, and C, were also found; these could be the consequence



6a

6b

Figure 6: A and B: Size and morphology of Silver Nanoparticle (AgNP) analysis by transmission electron microscopy by SEM (Figure 6a) and TEM (Figure 6b).

of plant extract that was either linked to the surface of AgNPs or adjacent to the particles to help with nanoparticle stabilization.¹⁷

Atomic force microscope

According to AFM measurements, the AgNPs, which varied in size between 3 nm to 10 nm, were comparable in shape. Figure 8 displays three-dimensional views of the AgNPs. The AgNPs' size and shape were examined using AFM analysis. According to the AFM images, the biosynthesized AgNPs had a tight size range and a majority of FCC shapes, as seen in Figure 4. The majority of the AgNPs were aggregated and ranged in size from 3 to 10 nm.¹⁸ Regarding the creation of AgNPs using a flower extract from *Cassia auriculata*. However, the synthetic NPs used in their studies were hexagonal, and a narrow, irregular size distribution was noted. AFM measured the particle size to be 42.01 nm. Figure 4 depicts the DLS (Dynamic Light Scattering) data, which reveals that the biosynthesized AgNPs' mean particle size was around 46.9 nm. Because the hydrodynamic radii of the NPs are measured by the DLS, a slightly high particle size value was discovered.

AgNP-induced cytotoxicity in MDA-MB-231 human breast cancer cells

The vitality of cells is a more significant aspect of the toxicological investigation in the assay to check how cells react to harmful substances and can offer details on metabolic processes, cell death, and cell survival. Cells were exposed to AgNPs at various concentrations varying from 2.5 to 15 g/mL, and toxicity was assessed to see how the AgNPs affected mitochondrial activity. The results of this experiment indicate that doses between 10 and 15 g/mL had a considerably greater effect on cell viability than values between 2.5 and 7.5 g/mL. AgNPs were discovered to be substantially hazardous to cells after 24 hr of treatment at concentrations of 12.5 g/mL and higher (Figure 9). Depending on the cell type and NP size, AgNP-given cells displayed reduced metabolic activity. On MDA-MB-231, The silver(colloidal)-induced in concentration-based cytotoxic activity. Size, shape,

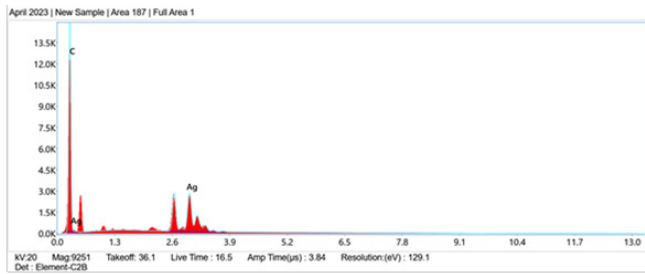


Figure 7: EDX spectrum of synthesized AgNPs/GC.

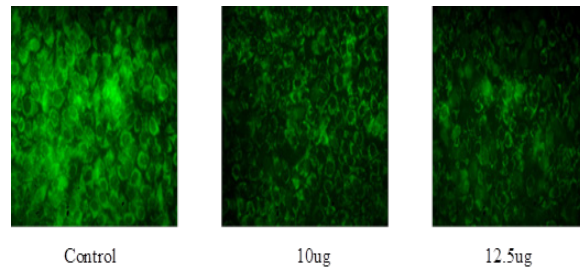


Figure 10: Effect of Silver Nanoparticles (AgNPs) on MMP activity in MDA-MB-231 human breast cancer cells.

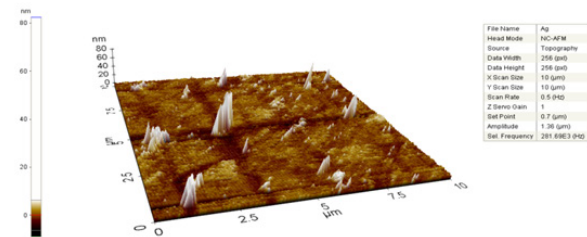


Figure 8: AFM 3D images.

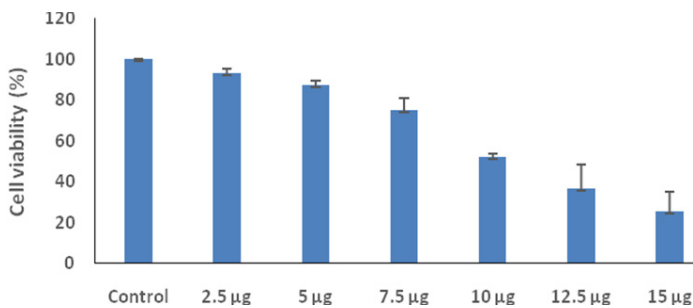


Figure 9: Cytotoxic effect of Silver Nanoparticles (AgNPs) on MDA-MB-231 human breast cancer cells. Cells were treated with AgNPs at various concentrations for 24 hr, and cytotoxicity was determined by the MTT (3-[4,5-dimethylthiazol-2-yl]-2,5-diphenyltetrazolium bromide) method.

media conditions, cell type, dose, and time dependency are all factors that affect how AgNPs act.¹⁹

Analysis of Mitochondrial Dysfunction

A recognizable indicator of cell death is rhodamine 123. The state of cells under a specific situation can be ascertained using the rhodamine 123 test. After giving the cells different AgNPs treatments for 24 hr, we looked at how different AgNPs concentrations affected the membrane's integrity. The findings imply that dosage dependence and significant effects on cell-membrane leakage were present (Figure 10). The Rhodamine 123 assay results supported the viability of the cells, and the cells

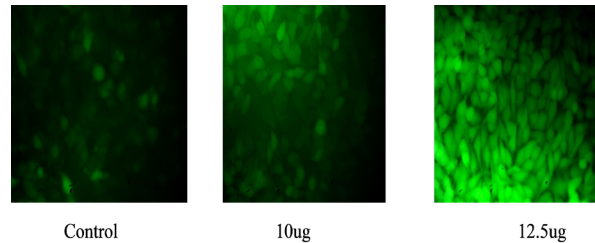


Figure 11: Silver Nanoparticles (AgNPs) induce Reactive Oxygen Species (ROS) generation in MDA-MB-231 human breast cancer cells. Relative fluorescence of 2',7'-dichlorofluorescein was measured.

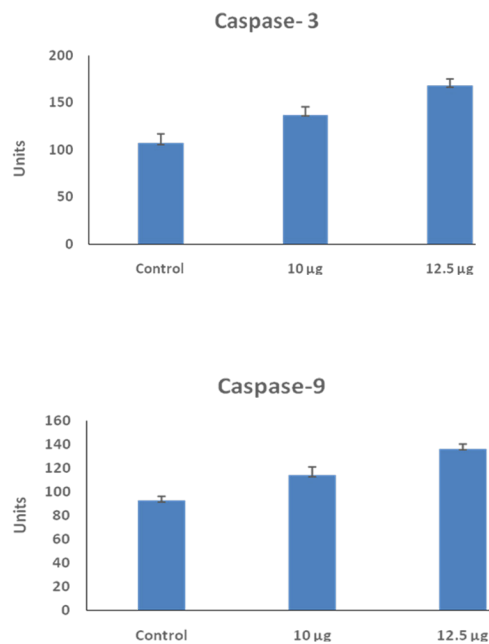


Figure 12: Silver Nanoparticles (AgNPs) induce the activity of caspase 3 and 9 in MDA-MB-231 human breast cancer cells. MDA-MB-231 cells were treated with AgNPs, Doxorubicin (DOX).

gradually grew more cytotoxic as AgNP concentrations were raised. The sudden cell-membrane lysis that caused the rise in LDH leakage ultimately resulted in cell death, suggesting that the membrane leakage was a side effect due to apoptosis. We discovered that an IC_{50} of 12.5 g/mL was adequate to cause cell death and significantly limit cellular growth. As a result, this concentration was used for more research.

AgNP-induced oxidative stress in MDA-MB-231

Various investigations have shown significant proof for establishing an association between AgNP-induced ROS generation and the development of oxidative stress and cytotoxicity. The formation of stress also leads a significant role in a range of cellular insults, including those that result in damage to the DNA and apoptosis.²⁰ AgNPs can generate ROS. Oxidative stress is the term for an abnormal buildup of ROS, which can seriously harm cells. A survey of the literature found the mechanism of AgNP-induced toxicity. We used the H₂DCF-DA test to assess ROS formation to determine how AgNPs affected oxidative stress. AgNP-induced formation of intracellular ROS was investigated by utilizing intracellular peroxide-dependent oxidation of DCFH-DA to create fluorescent DCF. The cells were treated with the positive control 1 M doxorubicin. DCF fluorescence was observed in cells treated with AgNPs. It is looked at ROS production which is frequently regarded as an essential element of apoptosis. The degree of ROS formation was noticeably higher in cells treated with AgNPs, which is agreeing with a rise in intracellular ROS (Figure 11). This study's findings suggest that ROS production alters the cellular redox level and is a cause of apoptosis.

AgNP-mediated caspase-3 and caspase-9 activation

AgNP-mediated genotoxicity and apoptosis have been demonstrated in several investigations using different types of cultured cells and also animal models. Apoptosis is a well-known unique form of programmed cell death in which cells are destroyed based on their genetic makeup. Effector molecules in apoptosis that are proteolytic enzymes, like caspases, are crucial. Caspases can be activated in response to environmental toxins by stimulating the intrinsic pathway or extrinsic pathway. Numerous regular biochemical processes depend on oxidative stress, and when these processes are abnormal, pathological processes result. Apoptosis is known to be brought on by a cell's excessive production of ROS (52 Several apoptotic mechanisms depend on the caspase-3 and 9 activation cascades. The cells were exposed to AgNPs to determine the impact of caspase-3 and 9 activations, and it is revealed that AgNPs induced cell death via apoptosis.²¹ Caspase 3 and 9 levels rose during treatment with AgNPs and doxorubicin, as seen in Figure 12. Caspase-3 and 9 play a significant part in the apoptotic process of cells, as evidenced by the fact that cells treated with caspase-3 and 9 inhibitors showed that caspase-3 and 9 activation was equivalent to control. The augmented activation of caspase-3 and 9 in AgNP-induced cells may play a role in apoptosis-related cell death. These data show that AgNPs cause apoptosis in breast cancer cells via caspase-3 and 9.²² The phytoconstituents of the *Psidium guajava*^{23,24} and *Ficus racemosa*²⁵ are consistent with the present investigation.

CONCLUSION

We used *Garcinia cambogia* extract, which is significant in the pharmaceutical industry, to demonstrate the formation of AgNPs and the mean size is 3 nm. In UV-visible spectra, these AgNPs had an absorption peak at 440 nm, which corresponded to the plasmon resonance of AgNPs. The involvement of mostly phenolic chemicals in the synthesis was revealed by FT-IR spectroscopy. The fabrication of politely even and monodisperse AgNPs was demonstrated by TEM and SEM, DLS findings. The production of silver was verified by the NPs' XRD spectra. Furthermore, toxicity tests supported the hypothesis that biologically produced AgNPs could be cytotoxic to MDA-MB-231 cells. Cell death and membrane leakage was seen in AgNP-treated cells in a concentration-dependent manner. The IC₅₀ was determined from the cell-proliferation assay to be 12.5 g/mL. Additionally, this study contends that AgNPs cause cell death by generating ROS and activating caspases-3 and 9. This study presents a new approach to curing several illnesses, including cancer, arthritis, and neurovascularization, by demonstrating the possible use of AgNPs for preventing the proliferation of cancerous cells and the cytotoxicity for possible healing in cancer therapy.

ACKNOWLEDGEMENT

The authors acknowledge PG and Research Department of Biochemistry, Bharathiyar University, Coimbatore, Tamil Nadu, India, for helping facility providing.

CONFLICT OF INTEREST

The authors declare that there is no conflict of interest.

ABBREVIATIONS

AgNPs: Silver Nanoparticles; **NPs:** Nanoparticles; **pH:** Potential hydrogen; **ROS:** Reactive Oxygen Species; **MMP:** Mitochondrial Membrane Potential; **PHF:** Fluorobenzene; **AgNO₃:** Silver nitrate; **TEM:** Transmission electron microscopy; **SEM:** Scanning electron microscope; **AFM:** Atomic Force Microscope; **DLS:** Dynamic Light Scattering; **DMEM:** Dulbecco's Modified Eagle Medium; **PBS:** Phosphate-buffered saline; **IC:** Inhibitory concentration; **DCF:** Dichlorofluorescein; **DCFH-DA:** Dichlorodihydrofluorescein diacetate; **NAC:** N-acetyl-L-cysteine; **FT-IR:** Fourier-transform infrared spectroscopy; **XRD:** X-ray diffraction; **LDH:** Lactate dehydrogenase; **MMP:** Matrix metalloproteinase.

REFERENCES

1. Samir K, Prabhat K, Chandra S, Chandra Shaker P. Silver micro-nanoparticles: properties, synthesis, characterization, and applications. *Intech Open*. 2021;266. doi: 10.5772/intechopen.99173.
2. Noga M, Milan J, Frydrych A, Jurowski K. Toxicological aspects, safety assessment, and green toxicology of silver nanoparticles (AgNPs)—critical review: state of the art. *Int J Mol Sci*. 2023;24(6):5133. doi: 10.3390/ijms24065133. PMID 36982206.
3. Ahmad F, Ashraf N, Ashraf T, Zhou RB, Yin DC. Biological synthesis of Metallic Nanoparticles (MNPs) by plants and microbes: their cellular uptake, biocompatibility,

- and biomedical applications. *Appl Microbiol Biotechnol*. 2019;103(7):2913-35. doi: 10.1007/s00253-019-09675-5, PMID 30778643.
4. John MS, Nagoth JA, Ramasamy KP, Mancini A, Giuli G, Natalello A, et al. Synthesis of Bioactive Silver Nanoparticles by a *Pseudomonas* strain Associated with the Antarctic Psychrophilic Protozoon *Euplotes focardii*. *Mar Drugs*. 2020;18(1):38. doi: 10.3390/md18010038, PMID 31947807.
 5. Padamsee TJ, Hills M, Muraveva A. Understanding low chemoprevention uptake by women at high risk of breast cancer: findings from a qualitative inductive study of women's risk-reduction experiences. *BMC Women Health*. 2021;21(1):157. doi: 10.1186/s12905-021-01279-4, PMID 33863327.
 6. Mundher AS, Naktal AD, Thokozani X, Ahmad R. Hot injection synthesis of orthorhombic SnS nanoparticles from Bis(O-n-Propyl)dithiocarbamate Diphenyltin(IV). *J Nano Res*. 2021;66:27-34. doi: 10.4028/www.scientific.net/JNanoR.66.27.
 7. Grzesiakowska A, Kasproicz MJ, Kuchta-Gładysz M, Rymuza K, Szeleszczuk O. Genotoxicity of physical silver nanoparticles, produced by the HVAD method, for *Chinchilla lanigera* genome. *Sci Rep*. 2021;11(1):18473. doi: 10.1038/s41598-021-97926-9, PMID 34531461.
 8. Ullah I, Khalil AT, Ali M, Iqbal J, Ali W, Alarifi S, et al. Green-synthesized silver nanoparticles induced apoptotic cell death in MCF-7 breast cancer cells by generating reactive oxygen species and activating caspase 3 and 9 enzyme activities. *Oxid Med Cell Longev*. 2020;2020:1215395. doi: 10.1155/2020/1215395, PMID 33082906.
 9. Ekaterina AL, Vetchinkina EP, Maria AK. Diversity of biogenic nanoparticles obtained by the fungi-mediated synthesis: a review. *Biomimetics*. 2023;8(1):1. doi: 10.3390/biomimetics8010001.
 10. Ji W, Shuduo X, Jingjing Y, Hanchu X, Yunlu J, Yulu Z, et al. The long noncoding RNA H19 promotes tamoxifen resistance in breast cancer via autophagy. *J Hematol Oncol*. 2019; 12(1):81. doi: 10.1186/s13045-019-0747-0.
 11. Rudrappa M, Kumar RS, Nagaraja SK, Hiremath H, Gunagambhire PV, Almansour AI, et al. Myco-nanofabrication of silver nanoparticles by *Penicillium brasilianum* NP5 and their antimicrobial, photoprotective and anti-cancer effect on MDA-MB-231 breast cancer cell line. *Antibiotics (Basel)*. 2023;12(3):567. doi: 10.3390/antibiotics12030567, PMID 36978433.
 12. Chunjiao L, YL, Yao L, Guanhua K, Yang C, Xuewei W, et al. Silver Nanoparticles cause neural and vascular disruption by affecting key neuroactive ligand-receptor interaction and VEGF signaling pathways. *Int J Nanomedicine*. 2023;18:2693-706. doi: 10.2147/2FIJN.S406184.
 13. Sarvesh RJ, Mansee T, Himanshu G. Biosynthesis of silver nanoparticles using mushroom extract and its toxicity assessment in zebrafish embryos. *Int J Plant Res*. 2022;36:119-26. doi: 10.1007/s42535-022-00483-3.
 14. Jitendra M, Uttariya P, Lakshika S, Amit KV, Monidipa G, Madan MS. Unveiling the cytotoxicity of phytosynthesized silver nanoparticles using *Tinospora cordifolia* leaves against human lung adenocarcinoma A549 cell line. *The Inst Eng Technol Nanobiotechnology*. 2020;14(3):230-8. doi: 10.1049/2Fiet-nbt.2019.0335.
 15. Adebayo EA, Azeez MA, Alao MB, Oke AM, Aina DA. Fungi as veritable tool in current advances in nanobiotechnology. *Heliyon*. 2021;7(11):e08480. doi: 10.1016/j.heliyon.2021.e08480, PMID 34901509.
 16. Arindam B, Bishnupada R, Pallab S, Paritosh M, Maloy K. M, Pranesh C, Shelley B, Ansuman C. Cytotoxic effect of green synthesized silver nanoparticles in MCF7 and MDA-MB-231 human breast cancer cells *in vitro*. *Nucleus*. 2019;63:191-202. doi: 10.1007/s13237-019-00305-z.
 17. Kumari R, Saini A, Chhillar A. K, Saini V, Saini R. Antitumor effect of bio-fabricated silver nanoparticles towards Ehrlich ascites carcinoma. *Bio interface Res Appl Chem*. 2021;11:12958-72. doi: 10.33263/briac115.1295812972.
 18. Yasser AS, Maha AA, Islam R, Mohamed H. A. Green synthesis of zinc oxide nanoparticles using aqueous extract of *Deverra tortuosa* and their cytotoxic activities. *Sci Rep*. 2020;10:3445. doi: 10.1038/s41598-020-60541-1.
 19. Kim D, Amatyra R, Hwang S, Lee S, Min KA, Shin MC. BSA-silver nanoparticles: A potential multimodal therapeutics for conventional and photothermal treatment of skin cancer. *Pharmaceutics*. 2021;13(4):575. doi: 10.3390/pharmaceutics13040575, PMID 33920666.
 20. Sun F, Li D, Wang C, Peng C, Zheng H, Wang X. Acacetin-induced cell apoptosis in head and neck squamous cell carcinoma cells: evidence for the role of muscarinic M3 receptor. *Phytother Res*. 2019;33(5):1551-61. doi: 10.1002/ptr.6343, PMID 31066474.
 21. Sony P, Kalyani M, Iyanar K. Antifungal activity of curcumin-silver nanoparticles against fluconazole-resistant clinical isolates of *Candida* species. *An Int Q J Res Ayurveda*. 2018;39(3):182-6. doi: 10.4103/ayu.ayu_24_18.
 22. Boice A, Bouchier-Hayes L. Targeting apoptotic caspases in cancer. *Biochim Biophys Acta Mol Cell Res*. 2020;1867(6):118688. doi: 10.1016/j.bbamcr.2020.118688, PMID 32087180.
 23. Manikandan R, Vijaya Anand A. Evaluation of antioxidant activity of *Psidium guajava* Linn. in streptozotocin-induced diabetic rats. *Free Radic Antioxid*. 2016;6(1):72-6. doi: 10.5530/fra.2016.1.9.
 24. Vijayakumar K, Rengarajan RL, Radhakrishnan R, Anand AV. Hypolipidemic Effect of *Psidium guajava* Leaf Extract against Hepatotoxicity in Rats. *Pharmacogn Mag*. 2018;14(53):4-8. doi: 10.4103/pm.pm_167_17, PMID 29576694.
 25. Khan A, Anand V, Badrinarayanan V, Thirunethiran K, Natarajan P. *In vitro* antioxidant and cytotoxicity analysis of leaves of *Ficus racemosa*. *Free Radic Antioxid*. 2016;7(1):8-12. doi: 10.5530/fra.2017.1.2.

Cite this article: Joseph MK, Indhumathi T. Synthesis of Functional Silver Nanoparticles and Microparticles with Modifiers and Evaluation of their Anti-cancer Activity on MDA-MB-453 Breast Cancer Cell Line. *Free Radicals and Antioxidants*. 2023;13(1):21-8.